N90-20926

ULTRASONIC TECHNIQUES FOR AIRCRAFT ICE ACCRETION MEASUREMENT * ^

R. John Hansman, Jr.,* and Mark S. Kirby†
Department of Aeronautics and Astronautics
Massachusetts Institute of Technology
Cambridge, Massachusetts

and

Fred Lichtenfelts ‡
Simmonds Precision
Aircraft Systems Division
Vergennes, Vermont

ABSTRACT

Results of tests to measure ice growth in natural (flight) and artificial (icing wind tunnel) icing conditions are presented. Ice thickness is measured using an ultrasonic pulse-echo technique. Two icing regimes, wet and dry ice growth, are identified and the unique ultrasonic signal characteristics associated with these different types of ice growth are described.

Ultrasonic measurements of ice growth on cylinders and airfoils exposed to artificial and natural icing conditions are presented. An accuracy of ±0.5 mm is achieved for ice thickness measurement using the pulse-echo technique. The performance of two-probe type ice detectors is compared to the surface mounted ultrasonic system. The ultrasonically measured ice accretion rates and ice surface condition (wet or dry) are used to compare the heat transfer characteristics for flight and icing wind tunnel environments. In general the heat transfer coefficient is inferred to be higher in the wind tunnel environment, not likely due to higher freestream turbulence levels. Finally, preliminary results of tests to measure ice growth on airfoil using an array of ultrasonic transducers are described. Ice profiles obtained during flight in natural icing conditions are shown and compared with mechanical and stereo image measurements.

1.0 INTRODUCTION

The direct measurement of ice thickness on critical aircraft surfaces, in flight and on the ground, has proven to be a difficult task. Current ice detectors generally measure the accretion of ice on a probe and infer the accretion on other aircraft components. In many applications this results in significant uncertainty as to the actual ice accretion on critical components. Recently, ultrasonic techniques have been developed which allow the ice accreted on critical components to be measured directly by a transducer imbedded in the surface. This technology has significant implications for operational use in measuring ice thickness and accretion rate in flight and automatically controlling ice protection systems. The technique also has potential applications in detecting hazardous ground icing events. In addition, ultrasonic techniques can be used to aid in the certification of aircraft for flight in icing condition and in understanding the physics which underlie the ice accretion problem.

The purpose of this paper is to present an overview of recent work on the measurement of ice thickness using ultrasonic pulse-echo techniques. Additional ultrasonic methods have been investigated including ice bond monitoring by shear wave techniques and thin ice detection by pulse-echo amplitude measurement. In the interest of brevity only the pulse-echo results will be reviewed here. Experimental measurements of ice growth in icing wind tunnel and flight icing conditions are presented. The ultra-sonic pulse echo technique is shown to provide the potential for the development of an operational instrument. In addition, the technique provides previously unobtainable resolution on the temporal and spatial growth of ice accretion in simulated and natural icing conditions. Finally, the unique capability of the ultrasonic pulse-echo technique to detect the presence of liquid water on an accreting ice surface allows the threshold between wet and dry ice growth to be experimentally determined. It is shown that this wet/dry threshold data may be used to infer valuable information about the heat transfer from the ice surface, and thus aid in understanding the ice accretion process.

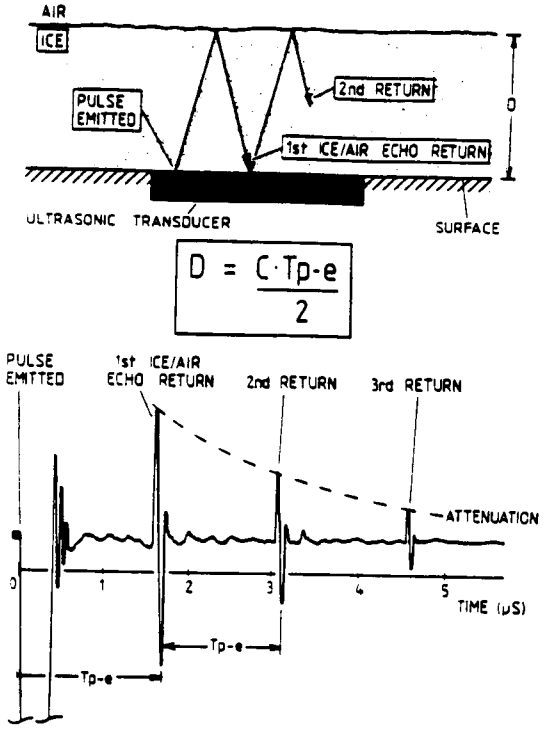

Fig. 1 Ultrasonic pulse-echo thickness measurement and typical ultrasonic pulse-echo signal in ice.

---

* Associate Professor, Member AIAA.
† Research Assistant, Currently at Rolls Royce, Bristol England.
‡ Lead Systems Engineer, Member AIAA.

*AIAA-84-4656-CP.
^Some original figures were not available at time of publication.

2.0 ULTRASONIC PULSE-ECHO MEASUREMENT TECHNIQUES.

2.1 ULTRASONIC PULSE-ECHO THICKNESS MEASUREMENT

Ultrasonic pulse-echo measurement of ice thickness on a surface is accomplished by emitting a brief compression or shear wave from a small ultrasonic transducer mounted flush with the accreting surface (Fig. 1). The pulse travels through the ice, is reflected at the ice/air interface and then returns to the transducer as an echo signal. The time elapsed, $T_{p\text{-}e}$, between the emission of the pulse from the transducer and the return of the echo from the ice interface can then be used to calculate the ice thickness, D, from the formula:

$$D = \frac{C \cdot T_{p\text{-}e}}{2} \qquad (1)$$

where C is the speed of propagation of the pulse-echo signal in ice. In a previous study[1], the speed of propagation was found to be insensitive to different types of ice (glaze, rime and mixed) formed at typical flight airspeeds. Fig. 2 illustrates the approximately constant speed of sound observed experimentally in ice samples formed under different icing conditions. A value of 3.8 mm/μs was used for the speed of sound in ice for all the results presented in this paper.

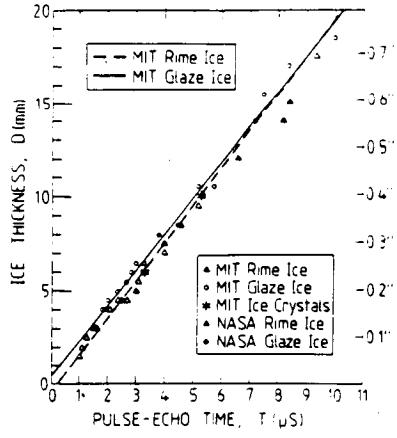

Fig. 2 Ice thickness vs. pulse-echo time constant speed of sound for ice samples formed under different icing conditions.

2.2 ULTRASONIC SIGNAL CHARACTERISTICS FOR DRY ICE GROWTH

In cold conditions, all the droplets impinging at a given location on a body freeze on impact and the ice surface formed are "dry". During dry ice growth, the ice surface tends to remain relatively smooth and simply increases in thickness. The received echo, therefore, appears to translate in time with a velocity proportional to the accretion rate. This behavior is illustrated in Fig. 3. Since the surface formed by dry ice growth is typically smooth, a sharp, well-defined echo is received, as shown in the figure.

2.3 ULTRASONIC SIGNAL CHARACTERISTICS FOR WET ICE GROWTH

In warm conditions at temperatures just below 0° C, the heat transfer from the accreting surface is insufficient to completely freeze all the impinging droplets and liquid water will be present on the ice surface. This form of ice accretion will be referred to as "wet ice growth", and is characteristic of glaze and mixed ice formation.

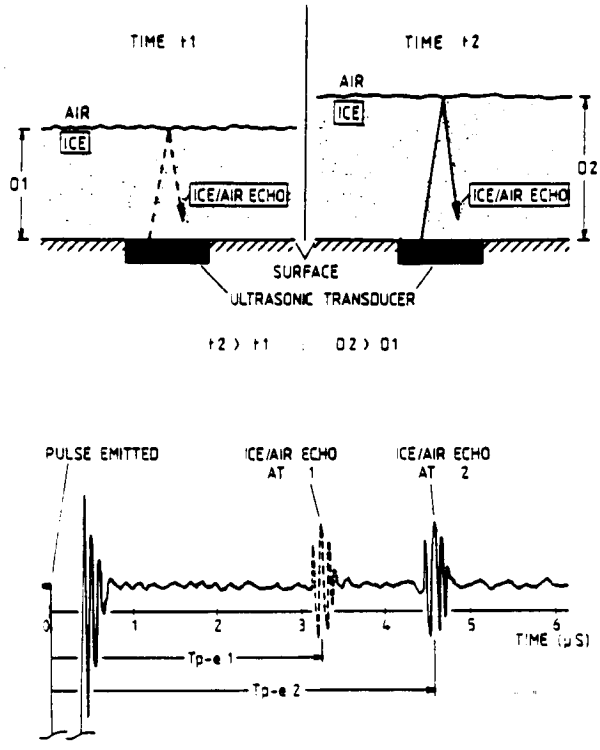

Fig. 3 Ultrasonic signal characteristics for dry ice growth.

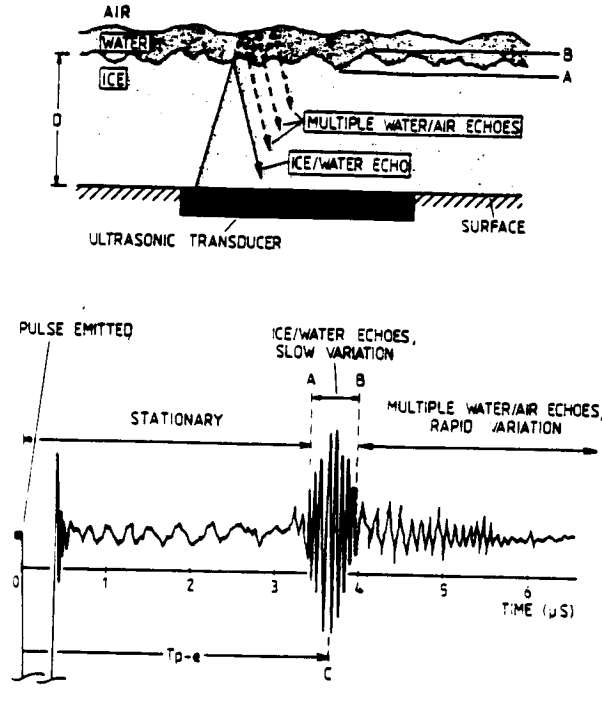

Fig. 4 Ultrasonic signal characteristics for wet ice growth.

During wet ice growth the ice surface is covered, at least partially, by a thin liquid layer. The ultrasonic pulse thus encounters two separate interfaces: an ice/water interface and a water/air interface, as shown in Fig. 4. Two echo signals are therefore received by the transducer; the first from the ice/water interface and a second, later echo from the water/air interface. The echo received from the ice/water interface is characteristically broader than the echoes received during rime ice growth due to the rougher ice surface formed during glaze icing. As in the rime ice case, this ice/water interface echo translates in time as liquid freezes at the interface and increases the accreted ice thickness.

Since the liquid layer over the ice surface is thin, and its attenuation is low, multiple echoes are received from the water/air interface following the ice/water echo. Due to distortion of the liquid surface by impinging droplets and the external flow, the detailed shape of these multiple water/air echoes changes rapidly as the instantaneous local thickness and surface orientation of the liquid layer varies. This rapid variation in the received echo signal is absent when the ice surface is dry. Wet and dry ice growth may thus be distinguished by observing the time variation of the received ultrasonic echo signals.

3.0 MEASUREMENT OF ICE GROWTH DURING ARTIFICIAL AND NATURAL ICING CONDITIONS

This section presents results of tests to measure and compare ice growth in both icing wind tunnel and icing conditions. Ice thickness on the stagnation line of a cylinder was measured as a function of the exposure time, using the ultrasonic pulse-echo technique in the NASA Lewis Icing Research Tunnel and on the NASA Icing Research aircraft. Preliminary tests of digitally processed "real time" ultrasonic measurement were conducted in the Boeing Icing Tunnel and on the Boeing 757 test aircraft. In addition, the ultrasonic signal characteristics were used to distinguish the presence of liquid water on the accreting ice surface. These wet/dry ice growth observations are then used to compare the heat transfer processes occurring in the icing wind tunnel and in flight.

3.1 EXPERIMENTAL APPARATUS

The experimental apparatus used for both the NASA Lewis Icing Research Tunnel (IRT) tests and the NASA natural icing flight tests consisted of the following equipment:

1. A cylinder containing small ultrasonic transducers mounted flush with the cylinder surface.

2. A pulser/receiver unit to drive transducers.

3. An oscilloscope to display the resulting pulse-echo signal.

4. A video camera/recorder to record the pulse-echo signal displayed on the oscilloscope.

Fig. 5 schematically illustrates the configuration of the experimental apparatus. For the IRT tests a 10.2 cm diameter cylinder was instrumented with four ultrasonic transducers. The transducers used had plane circular faces with element diameters of either 0.6 or 0.3 cm. The transducers had center frequencies of 1, 2.25 and 5 MHz; all were broadband, heavily damped transducers. As expected, the 5 MHz transducers provided the highest thickness resolution (due to the shorter wavelength), and all results presented are for 5 MHz transducers. The transducers were placed on the stagnation line and were located near the midsection of the cylinder. A pulser/receiver unit provided the electrical signals necessary to generate the ultrasonic pulse and amplify the return echo.

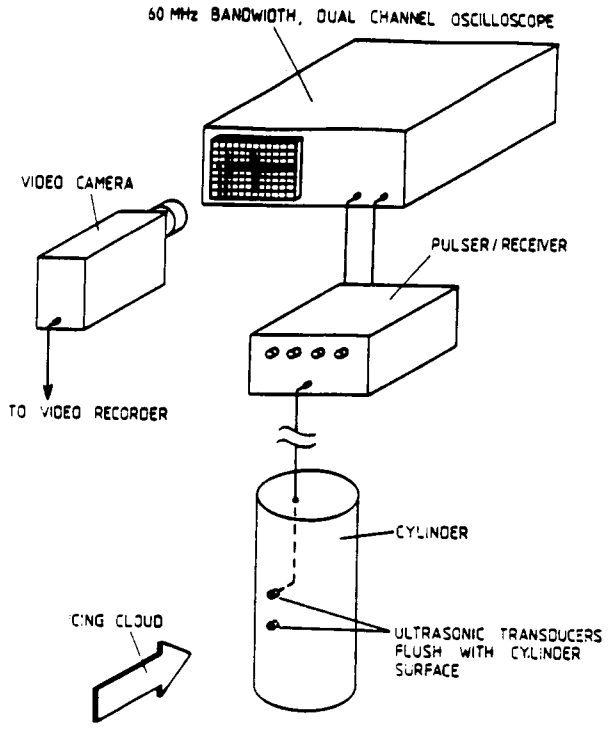

Fig. 5 Schematic of experimental apparatus configuration.

The cylinder employed for the NASA natural icing flight tests was an 11.4 cm diameter cylinder. This cylinder was instrumented with two 0.6 cm diameter, 5 MHz transducers, mounted in the stagnation line of the cylinder. Again a single pulser/receiver unit was used to drive either transducer.

In order to observe the ultrasonic signal characteristics in detail, an oscilloscope was used in both series of NASA tests to display the pulse-echo signals. A video camera was used to permanently record the oscilloscope signal for subsequent analysis. The video camera simultaneously recorded the cylinder exposure time from an electronic clock.

Preliminary tests of a digitally processed "real time" ultrasonic measurement techniques were conducted on a full scale model of a 757 leading edge slat in the Boeing Icing Tunnel. The slat was instrumented with commercially available 5 MHz transducers. Single and dual element transducers with polystyrene delay lines were tested. The diameter of the exposed polystyrene face was 0.63 cm. Transducer excitation and return echo signal conditioning was provided by commercial ultrasonic pulser/receiver hardware. A digital oscilloscope was used to capture return echoes and measure the round-trip delay. A micro-computer subsequently computed the ice thickness (approximately every 2.5 seconds) and logged the data on a printer. In addition, the oscilloscope pulse-echo waveforms were also video recorded to allow visual validation of the computer processing.

The Boeing natural icing flight tests used custom 2.25 MHz transducers with an exposed diameter of approximately 1.3 cm. One transducer was mounted on an outboard leading edge slat and another on a 7.6 cm diameter fared cylindrical shaped mast extended approximately 40 cm from the forwardmost passenger window as shown in Fig. 6. The transducers were connected to a modified commercial ultrasonic thickness gage which provided a digital display as well as an analog thickness output. In addition, echoes were monitored on an oscilloscope. Strip chart recordings were

made of the aircraft altitude, true airspeed, outside air temperature (OAT), liquid water content (LWC) and the analog ice thickness output. Visual observations of a wing mounted "barber-pole" were made to confirm the ice thickness readings.

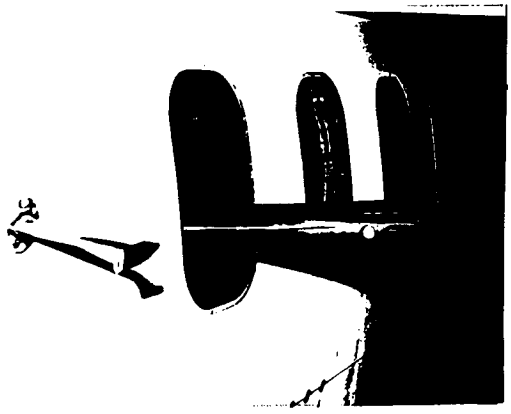

Fig. 6 Installation of the ultrasonic detector in the 757 window.

3.1.1 Icing Research Tunnel Tests

The instrumented cylinder was vertically suspended from the roof of the NASA Icing Research Tunnel (IRT), as shown schematically in Fig.7. The cylinder was exposed to the icing cloud, and the pulse-echo signals from the transducers being compared recorded using the video-camera/recorder. Each exposure was made with constant icing cloud parameters and typically lasted eight minutes. At the completion of a run, the iced diameter of the cylinder at each transducer located was measured mechanically using a pair of outside calipers. The ice thickness over the transducers was inferred from this measurement for comparison with the ultrasonically measured ice thickness. The cylinder was then completely de-iced in preparation for the next run. Ice growth for a total of fifteen different icing cloud parameter sets, ranging from glaze to rime icing conditions, was recorded using the ultrasonic pulse-echo system.

3.1.2 Boeing Icing Tunnel Tests

The 757 leading edge model spanned the tunnel at approximately a 20° sweep angle. A total of 20 tests were conducted. The test conditions covered a temperature range of -28° C to +2° C; LWC of 0.2 to 0.9 gm/m^3 and airspeed from 100 to 175 MPH. Droplet size (MVD) was gravitational 10 or 20 microns, depending upon LWC. The exposure time varied from two to 15 minutes. Typically ice was allowed to accrete until between 0.150 to 0.300 inches were present. The tunnel was then opened and a manual measurement of the ice thickness over the transducer was made using calipers.

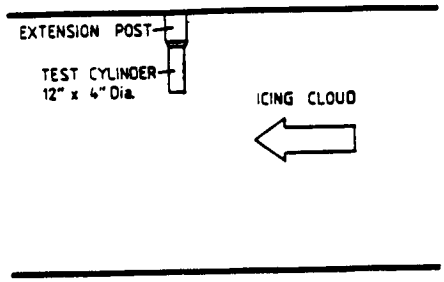

Fig. 7 Test cylinder installation for icing tunnel (IRT) tests.

3.1.3 Natural Icing Tests

Natural icing tests were conducted in flight from the NASA Lewis Icing Research Aircraft, a De Havilland Twin Otter. The 11.4 cm cylinder instrumented with ultrasonic transducers was exposed to icing conditions at the end of an extension post that was vertically extended through the roof of the aircraft by an experiment carrier mounted in the aircraft (see Fig.8). The cylinder midsection was located 53.3 cm into the freestream when extended. The cylinder was typically exposed throughout the entire icing encounter, the pulse echo signal again being continuously displayed and recorded by the oscilloscope/camera system. At the end of the encounter the cylinder was retracted into the aircraft and the ice thickness over the transducer measured using outside calipers. Four research flights were conducted with the ultrasonic system during the period March 30 to April 2, 1985.

The Boeing 757 flight tests were conducted on February 28, 1987 from Boeing Field in Seattle. Four icing encounters occurred at an altitude of approximately 10,000 ft. Each encounter lasted from five to nine minutes and was terminated by climbing above the icing conditions. Following the last encounter, total ice accumulation was in excess of one inch. The transducer mounted on the mast accurately tracked ice accretions in excess of 1 inch. The slat mounted transducer failed to perform as expected. This is thought to be due to an inadequate transducer mounting arrangement which prevented the direct bonding of accreted ice to the sensor.

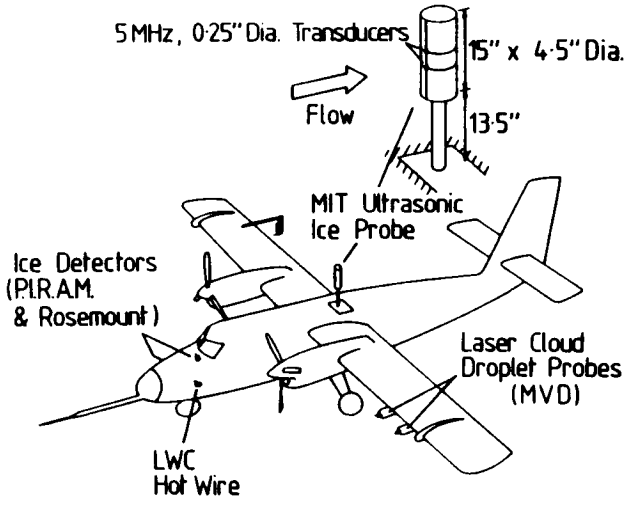

Fig. 8 Test cylinder installation for natural icing (NASA Lewis Twin Otter aircraft) tests.

3.2 RESULTS AND DISCUSSION

3.2.1 Icing Research Tunnel Tests

Figs. 9 and 10 show ice thickness measured with the ultrasonic system plotted against exposure time for two different icing cloud parameter sets, labeled "heavy" and "light" icing respectively. The heavy icing conditions represent an icing cloud with a high liquid water content of approximately 0.77 gm/m^3 and a large median volume droplet size of 20 microns; whereas the light icing conditions represent relatively lower values for both of these parameters. The freestream airspeed was 102.8 m/sec for both cases shown. Ice growth at three different temperatures (-8.0° C, -17.5° C and -28.6° C), is shown for both icing conditions.

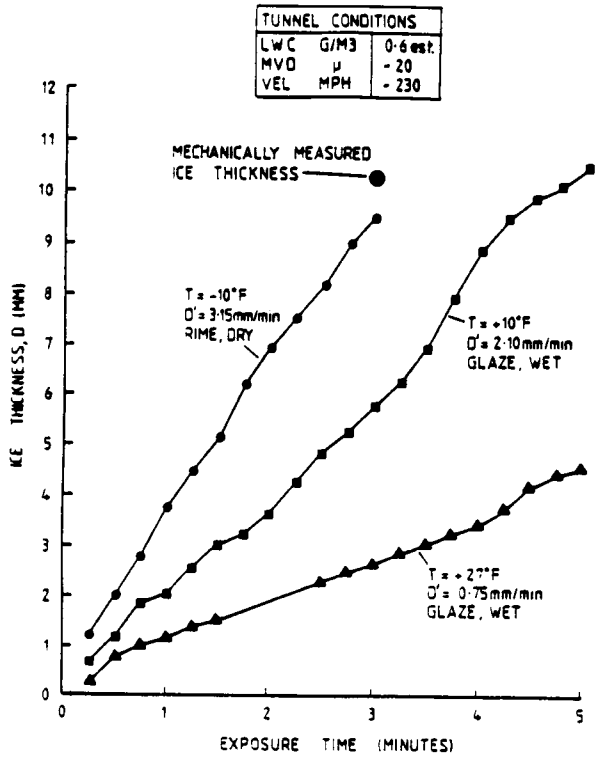

Fig. 9 Ice growth under "heavy" icing tunnel conditions.

The total ice accretion was mechanically measured with outside calipers at the completion of each run and is also plotted, if known. The accuracy of the ultrasonic pulse-echo thickness measurements was found to be within 0.5 mm of the accretion measured with the calipers for all runs where mechanical measurements were obtained. This good agreement between the mechanically measured thicknesses and the ultrasonic measurements confirmed previous experimental results which showed the speed of propagation of the ultrasonic signal to be insensitive to widely varying icing conditions.

The ice accretion rates measured in the IRT (given by the slope of the thickness versus time curve) remained fairly constant throughout each run. This behavior is a result of both the constant icing cloud conditions in the tunnel and the location of the transducer on the cylinder stagnation line

While observed accretion rates are relatively constant throughout each run, the accretion rates differ significantly for the different icing cloud conditions. Due to the higher impinging mass flux, the accretion rates measured under the "heavy" icing conditions were greater than those observed under the "light" icing conditions at the same temperature. For example at -28.6° C the accretion rate is 3.15 mm/min for the heavy icing conditions while it was only 1.05 mm/min for the "light" icing case. Of more interest is the effect of the cloud temperature on the stagnation accretion rate. At the relatively warm temperatures just below 0° C, the accretion rates for both the heavy and light cases are low, and the ice growth is observes to be wet. Under these conditions, the rate of heat removal from the ice surface was sufficient to completely freeze all the locally impinging droplets, liquid forms on the accreting surface and ran back away from the stagnation region. However, as the temperature of the icing cloud was progressively reduced, the accretion rate was observed to increase to a maximum value and then remain constant despite further decreases in icing cloud temperature.

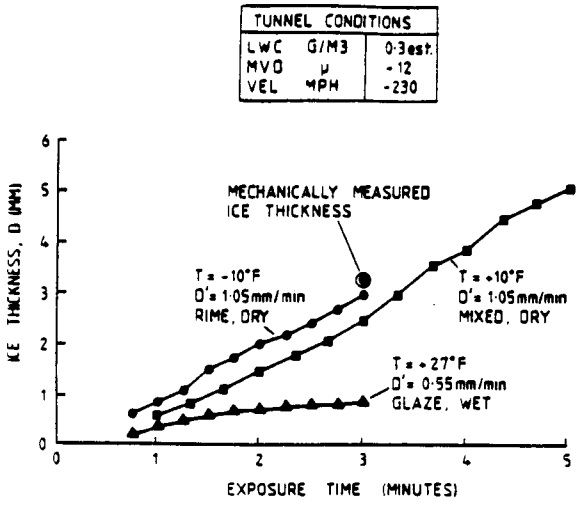

Fig. 10 Ice growth under "light" icing tunnel conditions.

The lower accretion rates observed at the warmer cloud temperatures are due to liquid runback from the stagnation region. As the cloud temperature is reduced, the rate of heat removed from the ice surface increases, this results in the freezing fraction (ratio of impinging to freezing water flux) and the accretion rate increasing. For dry growth, the freezing fraction is unity and the accretion rate is a maximum (for the particular cloud parameters). This behavior is illustrated in Fig. 11, which shows the average accretion rates measured for the heavy and light icing conditions as a function of the cloud temperature, T_∞. For the light icing case the accretion rate increases with decreasing temperature to -17.5° C, at which point dry ice growth is observed, the accretion rate then remains constant as the icing cloud temperature is further decreased to -28.6° C. However, for the heavy icing conditions it can be seen that at -17.5° C the growth is still wet and the accretion rate continues to increase from -17.5° C to -28.6° C. For these "heavy icing" conditions the heat transfer from the ice surface as still insufficient at -17.5°C to completely freeze the high impinging mass flux, and hence wet growth was observed. At -28.6° C though the ice growth is dry and the accretion rate measured, 3.15 mm/min is therefore the maximum value for those conditions.

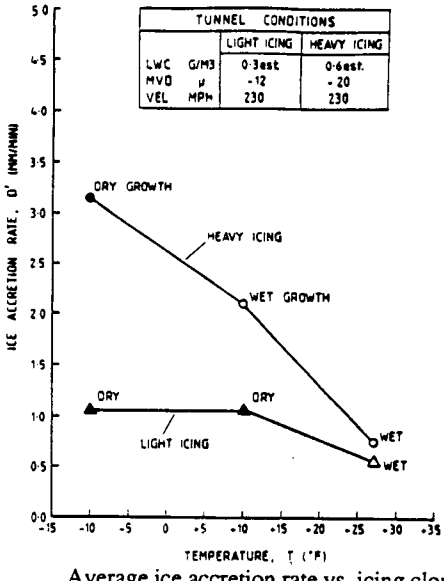

Fig. 11 Average ice accretion rate vs. icing cloud temperature for "heavy" and "light" icing tunnel conditions.

3.2.2 Boeing Icing Tunnel Tests

Fig. 12 shows an example of ice thickness measured and processed in real time with the digitally analyzed ultrasonic data. As can be seen in the data, the preliminary algorithms used in this test required approximately 0.075" of ice before it locked in. However, a clear reaction in the echo amplitude was always observed within 5 seconds of spray initiation. This amplitude behavior has been subsequently used for ultrasonic measurement of thin ice accretions. The agreement between final ultrasonic and mechanical ice thickness measurements was generally good with most cases agreeing to better than 10%. Those outliers which did occur were trackable to problems with the preliminary signal processing algorithm.

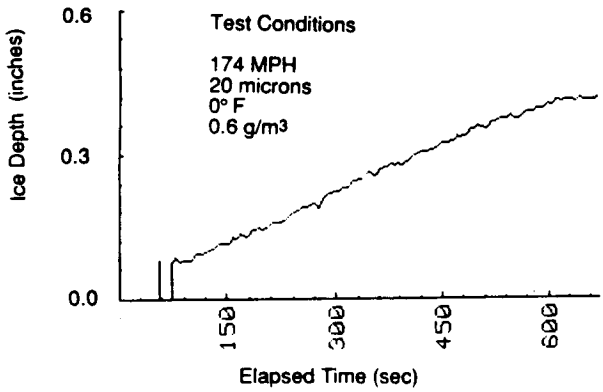

Fig. 12 Digitally processed ice growth measurement.

3.2.3 Natural Icing Tests

Fig. 13 contains a summary of the time averaged icing conditions during each of the four in-flight exposures of the ultrasonic system obtained on the NASA Icing Research Aircraft. The shape of the accreted ice at the completion of each exposure was obtained from photographs of the iced cylinder. Also shown are the final ice thicknesses measured with the ultrasonic system and the outside calipers. The accuracy of the ultrasonic measurements is again seen to be within ±0.5 mm of the mechanically measured ice thickness.

Fig. 14 is a plot of the ice thickness measured with the ultrasonic system versus the cylinder exposure time, for research flight 85-24. Ice pulse-echo data, and the average accretion rate for the encounter was 0.88 mm/min.

Fig. 15 is a plot of icing cloud and ice accretion data measured by existing instrumentation on the aircraft, also for flight 85-24. The upper plot shows "icing rate" in mm/min measured by Rosemount and PIRAM ice detectors. Also shown is the ice accretion rate measured on the stagnation line of the test cylinder by the ultrasonic system. This accretion rate was determined by differentiating the measured ice accretion (Fig. 14) with respect to time. The lower plot shows the cloud liquid water content in gm/m^3 measured by a Johnson-Williams hot-wire probe. Due to the relatively cold cloud temperature and low liquid water contents observed during this encounter, the icing rate is expected to be approximately proportional to the cloud liquid water content.

From Fig. 15, it can be seen that three icing rate plots (Rosemount, PIRAM and Ultrasonic) show overall similarity to the LWC plot, (e.g., all contain a decrease in icing rate after two minutes, corresponding to a decrease in the cloud liquid water content). However, the magnitudes of the icing rates indicated by the three instruments are markedly different, the PIRAM and Rosemount respectively indicating average icing rates of 2.45 and 1.96 mm/min for the encounter while the

TIME - AVERAGED ICING CONDITIONS						
FLIGHT NUMBER	EXPOSURE TIME (MIN:SEC)	TEMP (°F)	LWC (GM/M3)	MVD (μ)	VEL (MPH)	ALTITUDE (FEET)
85-22	20:41	+22.3	0.36	11.9	157	2728
85-23	47.08	+26.1	0.18	11.4	147	3404
85-24	10.07	+5.7	0.46	14 est.	161	6480
85-25A	36:40	+4.8	0.19	14.1	167	7019
85-25B	11.29	+8.8	0.12	12.0	167	6837

FLIGHT NUMBER	ULTRASONICALLY MEASURED ICE THICKNESS (MM)	MECHANICALLY MEASURED ICE THICKNESS (MM)	ICE SHAPE
85-22	3.1	2.7	TRANSDUCER, FLOW, WET GROWTH
85-23	3.3	ICE SLID OFF	WET
85-24	8.9	8.7	DRY
85-25A	VIDEO TAPE DAMAGED	9.6	DRY
85-25B	1.0	1.3	DRY

Fig. 13 Summary of natural icing test results.

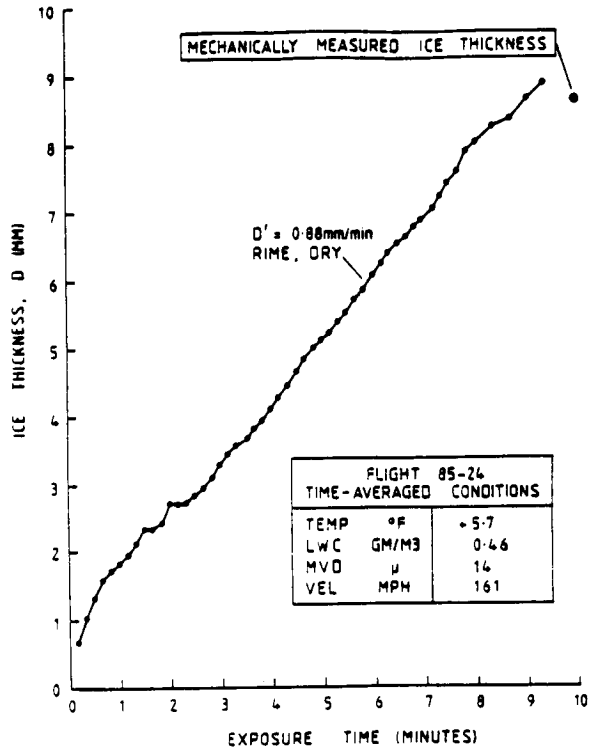

Fig. 14 Ice thickness vs. exposure time for flight 85-24.

average ultrasonically measured accretion rate is 0.88 mm/min. The ultrasonically measured icing rate is consistent with the mechanically measured accretion on the test cylinder of 8.7 mm at the end of the ten minute exposure. The higher icing rates recorded by the PIRAM and Rosemount systems appear to be inconsistent with the cloud liquid water content measured by the Johnson-Williams probe, a regression line analysis of measured icing rate versus Johnson-Williams cloud liquid water content was made which indicate that the PIRAM and Rosemount systems respectively imply icing rates of 2.06 and 1.36 mm/min at zero liquid water content.

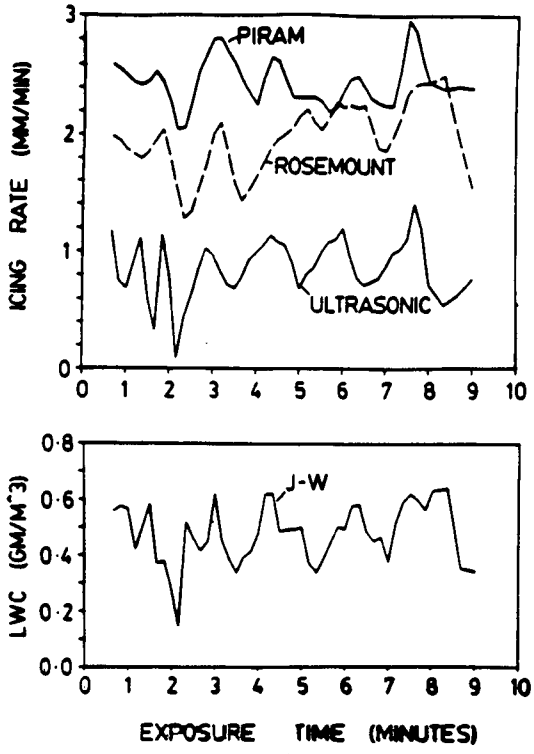

Fig. 15 Comparison of ice accretion rates measured by PIRAM, Rosemount and ultrasonic ice detectors and cloud liquid water content measured by a Johnson-Williams hot-wire probe for flight 85-24.

The PIRAM and Rosemount systems are both probe-type detectors that measure ice accumulation on a small, protruding probe. The calibration of these systems depends on the collection efficiency of the probe, which in turn varies with the cloud droplet size distribution. Since the ultrasonic system is non-invasive, ice thickness and icing rate are directly measured on the surface of interest and no calibration is required. Referring again to Fig. 15, it can be seen that the time variation of the liquid water content is recorded by the ultrasonic system while the Rosemount and PIRAM plots do not contain the same level of detail, particularly beyond four minutes exposure time, with the Rosemount data showing an apparent drift to a higher icing rate. The time response of probe-type systems is generally limited by two factors: the amount of ice necessary to initiate the icing signal and the need to repeatedly thermally de-ice the probe. The response time of both the PIRAM and Rosemount instruments is therefore dependent on the severity of the icing conditions and also physically limited by the time taken to de-ice the probe (typically 5-7 seconds). The time response of the ultrasonic system is not limited by the need for de-icing and does not depend on the icing severity; it is only fundamentally limited by the ultrasonic pulse repetition frequency, which is typically several KHz.

Fig. 16 presents strip chart data from an 8 minute period of the 757 flight test. The ultrasonically measured ice accretion is the bottom trace in Fig. 16. The measured ice accretion behavior is consistent with the measured liquid water content, also shown in Fig. 16. Reliable measurements were made to greater than 0.75 inches before the detector saturated. The average ambient temperature during the encounter was -15° C, the pressure altitude was 10,000 ft. and the true airspeed was 250 KTS.

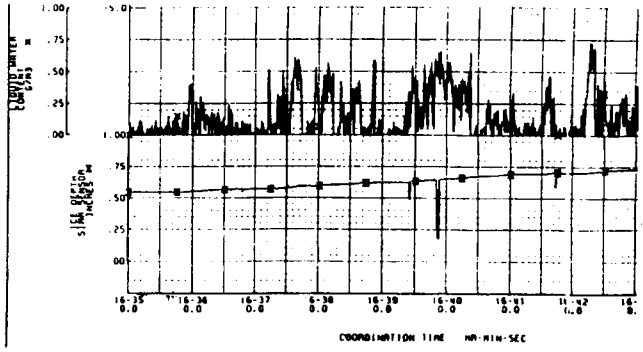

Fig. 16 Example of strip chart recordings of cloud liquid water content and ultrasonically measured ice thickness for the Boeing 757 tests.

3.3 HEAT TRANSFER MEASUREMENTS FOR AN ACCRETING ICE SURFACE

As discussed earlier, when the rate of heat removal from the icing surface is insufficient to freeze all the impinging droplets, liquid will form on the surface and the ice growth will be wet. By experimentally measuring the type of ice growth occurring (wet or dry) under particular icing cloud conditions, it is possible to parametrically infer limits on the heat transfer magnitude at the icing surface. A clear understanding of the heat transfer is essential if accurate analytic ice accretion models are to be developed. Due to experimental difficulties associated with heat transfer measurements on actual ice surfaces, local heat transfer coefficient measurements have only been made around wooden or foam models of typical ice shapes. In addition, experimental measurements comparing local heat transfer coefficients obtained in icing wind tunnels and in flight are essential if natural icing conditions are to be accurately simulated in icing wind tunnels. Very little experimental data exists in this area.

This section presents a comparison of experimentally measured wet and dry ice growth data with theoretical wet/dry threshold curves calculated using a steady-state energy balance for the stagnation region. The energy balance shown in Fig. 17 considers six modes of energy transport to and from the icing surface, the most significant terms being the heat added due to the latent heat of fusion and aerodynamic heating ("ram-rise"). The heat is removed primarily due to convection and evaporation or sublimation. The ultrasonically measured wet and dry ice growth data for the cylinders tested in the icing wind tunnel and in flight are used to compare a series of heat transfer coefficients for the cylinder stagnation region. Using this approach, the importance of freestream turbulence and surface roughness on the local heat transfer can be compared for artificial and natural icing conditions.

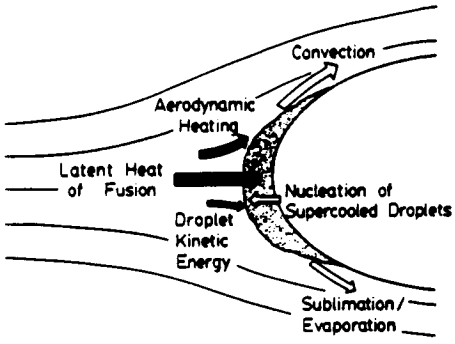

Fig. 17 Modes of energy transfer for an accreting ice surface.

The heat transfer coefficients used are from a recent experimental study by Van Fossen, et al[2], in support of the NASA icing research program. In the Van Fossen study, heat transfer coefficients were measured for two different freestream turbulence levels, 0.5% and 3.5%, and for two different cylinder surface conditions, one smooth and one roughened with grains of sand. A more complete discussion of these heat transfer models and the steady-state energy balance used to calculate the wet/dry threshold curves is contained in reference 3.

3.3.1 Icing Research Tunnel Results

Fig. 18 shows the ultrasonically measured ice growth for six different icing conditions in the icing research tunnel. The freestream velocity was 102.8 m/s (230 mph) for all six runs shown. Also shown are four wet/dry threshold curves calculated using the Van Fossen[3] heat transfer coefficients. These curves are plotted versus ambient temperature and were calculated for a freestream velocity of 102.8 m/s (230 mph), and a cylinder diameter of 0.102 m (4 in). The four curves shown thus represent the transition between wet and dry ice growth calculated for the four different local heat transfer coefficients implied by the Van Fossen data. If the local impinging liquid water content exceeds this critical value for a given ambient temperature then the ice growth is calculated to be wet, and if the impinging liquid water content is less than the critical value the ice growth is predicted to be dry. From the figure it can be seen that the heat transfer coefficient that best predicts the experimentally observed pattern of wet and dry ice growth is that measured for the cylinder roughened with sand and at a freestream turbulence level of 3.5%. While dry ice growth was observed at -28.6°C and an impinging liquid water content equal to 0.47 g/m^3, the heat transfer coefficients for the 0.5% freestream turbulence level clearly imply wet growth for these conditions. Thus it appears that the 0.5% turbulence level heat transfer coefficients underpredict the actual heat transfer in the icing tunnel, and are therefore too low.

Since the rough surface, 3.5% freestream turbulence heat transfer coefficient appeared to best approximate the actual heat transfer occurring in the icing research tunnel (based on the wet/dry ice surface data from th ultrasonic tests), this heat transfer model was compared with other ultrasonic wet/dry ice surface data obtained at different tunnel icing cloud conditions, with similarly favorable results.

Based on the results presented in Fig. 18, it appears that the heat transfer coefficient model that best approximates the actual heat transfer occurring in the icing research tunnel is the 3.5% turbulence level, rough surface model. The actual heat transfer coefficient is clearly greater than those applicable at the low (0.5%) turbulence level and may be even greater than that implied by the high (3.5%) turbulence level model.

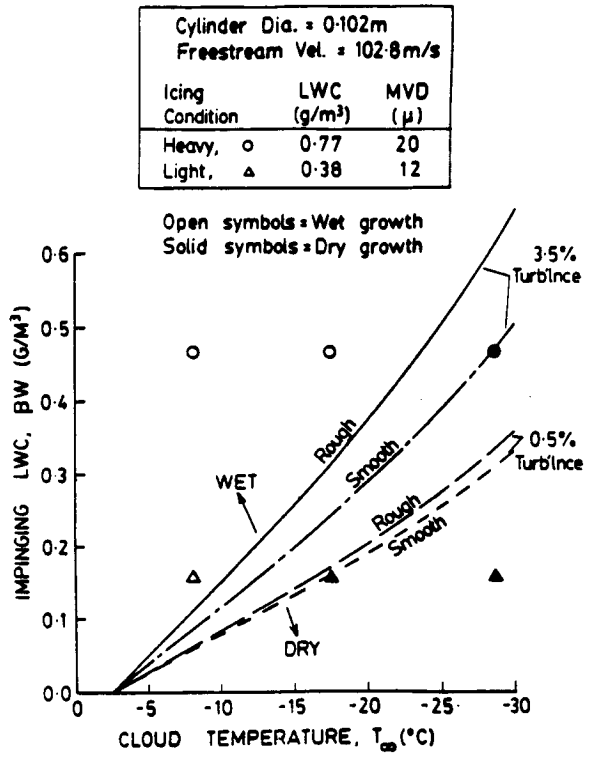

Fig. 18 Plot of impinging liquid water content vs. cloud temperature showing ultrasonically measured wet/dry ice growth and theoretical wet/dry threshold curves for four different heat transfer coefficients (V_∞= 102.8 m/sec.).

3.3.2 Natural Icing Cloud Test Results

While constant icing conditions were maintained throughout each exposure in the icing research tunnel, the natural icing cloud conditions, most noticeably the liquid water content, were not constant throughout each flight. Fig. 19 shows a plot of cloud liquid water content versus exposure time for research flight 85-24. The liquid water content was measured by a Johnson-Williams hot-wire probe located near the nose of the aircraft (see Fig. 8). Also shown, are the experimentally observed periods of dry, wet and transitional ice growth, produced by the varying liquid water content. The ultrasonic echo patterns received from the accreting ice surface were used to determine if the ice growth was wet, dry or transitional. Ice growth was characterized as transitional when the time variation of the ultrasonic echo pattern was between that characteristically observed for wet and completely dry ice growth.

Fig. 20 is a plot of impinging liquid water content versus cloud temperature. The experimentally observed ice growth regimes during the four research flights conducted are shown. Note that during flights 85-24 and 85-25 the full range of ice growth regimes were encountered with periods of dry, transitional and wet ice growth observed. No dry ice growth was observed during flights 85-22 and 85-23. Also shown are the four wet/dry threshold curves calculated using the four different Van Fossen heat transfer coefficients (0.5% turbulence, rough and smooth surface; 3.5% turbulence, rough and smooth surface). These curves were calculated for the test cylinder diameter of 0.114 m and for the average flight airspeed of 71.4 m/s and the average exposure altitude of 1613 m.

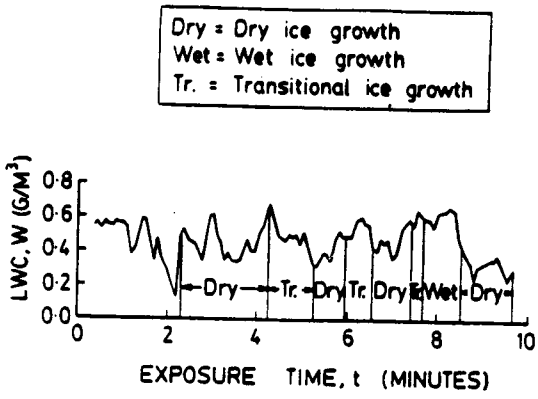

Fig. 19 Plot of liquid water content (measured by the Johnson-Williams probe) vs. exposure time for flight 85-24 showing typical fluctuations observed in natural icing conditions. Also shown are ultrasonic measured periods of wet, dry, and transitional ice growth.

Figs. 19 and 20 illustrate the considerable variations encountered in natural icing conditions, both during a particular flight and between flights conducted on different days. For example, the cloud temperature, liquid water content and droplet size were roughly comparable for flights 85-24 and 85-25. However, different ranges of wet and dry ice growth were observed, as indicated by the overlapping experimental wet and dry growth ranges at the same impinging liquid water content. The implication is that the heat transfer differed between the two flights, both at nominally similar icing conditions, but conducted on different days through different clouds.

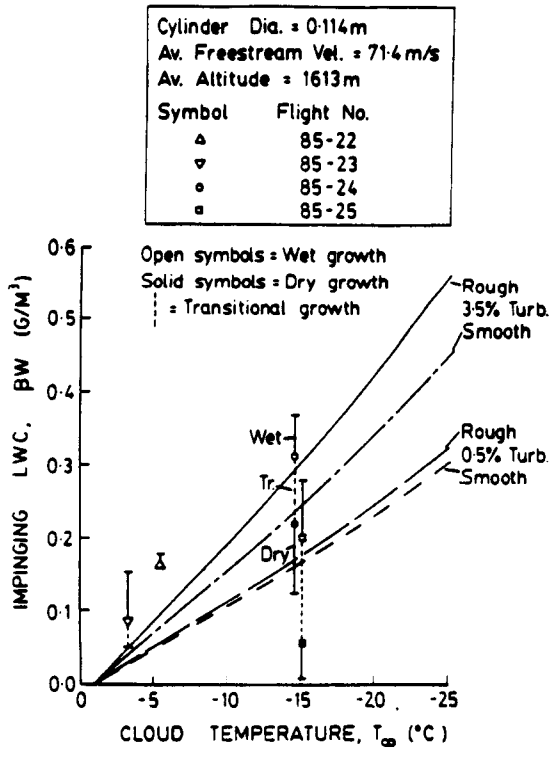

Fig. 20 Plot of impinging liquid water content vs. cloud temperature showing wet, dry and transitional ice growth regimes observed in flights and theoretical wet/dry threshold curves for four different heat transfer coefficients.

From the figure it can be seen that for flight 85-25 the high (3.5%) turbulence level heat transfer coefficients overpredict the observed heat transfer, based on the steady-state model analysis. For this flight the low (0.5%) turbulence level heat transfer coefficients appear appropriate since both of these coefficients correctly predicts the observed wet and dry regimes. The actual turbulence level applicable could be even less than 0.5% based on the location of the observed wet and dry growth regimes.

The experimentally observed ice growth regimes during flight 85-24 are consistent with the wet/dry threshold predicted by the 3.5% turbulence level, rough surface heat transfer coefficient. For this flight the low (0.5%) turbulence level models incorrectly predict wet growth for impinging liquid water content levels where dry growth was experimentally observed. Thus, in contrast to flight 85-25, the low turbulence level appears to be too low, and the 3.5% turbulence level model gives acceptable results.

The results of the natural icing tests also indicate the heat transfer occurring in natural icing conditions may vary from day to day despite similar icing conditions. One reason for this variation may be due to different icing cloud turbulence levels. Based on the limited amount of flight test data available it appears that in general the appropriate turbulence level for natural icing conditions is somewhat lower than the 3.5%+ level inferred for the icing research tunnel. This result is consistent with previous experimental comparisons between the icing research tunnel and flight. For these reasons, care should be taken in extrapolating the results of icing wing tunnel tests to "similar" natural icing cloud conditions.

4.0 MEASUREMENT OF ICE SHAPE BY AN ULTRASONIC ARRAY

Currently a comprehensive testing program is under way to measure and compare ice accretion in natural and artificial wind tunnel icing conditions. This ice-growth data base will enable a quantitative comparison to be made between flight and icing wind tunnel tests. In addition, this temporal and spatial ice accretion data will be used to support development and validation of analytic icing models and scaling laws. This section describes the experimental apparatus and testing procedure for these tests, and presents preliminary results of ice growth measurements made on an airfoil in natural icing conditions[4].

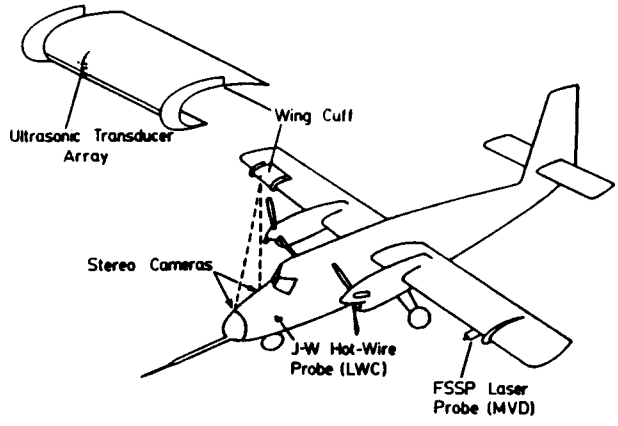

Fig. 21 Wing-cuff and ultrasonic array installation on NASA Lewis Twin Otter aircraft.

4.1 EXPERIMENTAL APPARATUS

For the natural icing flight tests a De Havilland DHC-6 airfoil section was instrumented with an array of 9 ultrasonic transducers, as shown in Fig. 21 The transducers were all 5 MHz, broadband, heavily damped transducers with 0.6 cm element diameters. The airfoil section was attached to the starboard wing of the NASA Lewis Icing Research Aircraft, a De Havilland DHC-6 Twin Otter. The airfoil section, or cuff, thus protruded approximately 3 in forward of the aircraft wing section.

The NASA aircraft was also equipped with a stereo camera system consisting of two 70 mm cameras mounted in the nose of the aircraft (see Fig. 21). The cameras produce stereo image pairs of the ice accretion on the wing cuff. These images are then photogrammetrically analyzed post-flight, and allow the ice accretion to be measured with a resolution of approximately ±0.03 in.

Fig. 22 schematically illustrates the ultrasonic system installation for the natural icing flight tests. The 9 ultrasonic transducers in the wing cuff were sequentially scanned using a multiplexing pulser/receiver unit. The pulse-echo signals were displayed on a broadband oscilloscope and a video camera focused on the oscilloscope screen provided a permanent record of these signals. Also within the camera's field of view were an electronic watch to provide time synchronization with other icing data recorded onboard the aircraft, and an LED display to indicate the current active transducer in the array.

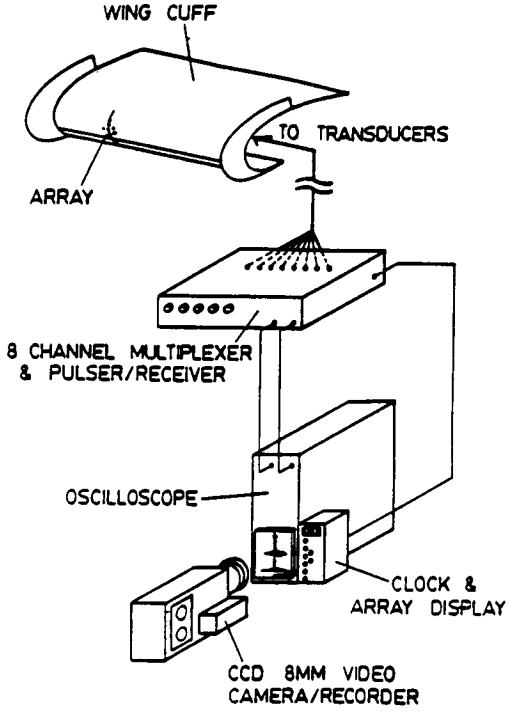

Fig. 22 Schematic of ultrasonic array equipment configuration.

4.2 TESTING

Since the instrumented wing cuff was permanently exposed on the aircraft wing, the ultrasonic system was activated from take-off to landing. Typically the multiplexing rate was set to approximately two seconds per transducer (i.e., each transducer was "active" for two seconds), so that four complete scans of the array were completed every minute.

In addition to the ultrasonic ice thickness measurements, stereo photographs of the wing cuff accretion were also taken during each encounter. However, adequate stereo photographs could not be obtained while the aircraft was inside the icing cloud, stereo photographs of the ice growth were therefore only taken outside the cloud at fairly widely spaced time intervals. Typically two or three separate stereo pairs were obtained documenting the ice growth during the icing encounter.

Since the wing cuff was not equipped with any ice protection system, in most cases it was possible to mechanically measure the final ice accretion on the wing cuff after landing using vernier calipers. Nine research flights were conducted with the ultrasonic system during the period February to March 1986. Due to the weather conditions during that period rime ice accretions were observed primarily.

4.2.1 Results

Fig. 23 shows a typical ice growth profile history obtained from the ultrasonic array. The data were from research flight 86-31 which had a cold average temperature of -10° C and a low liquid water content of 0.06 g/m^3. The data are presented in the form of successive ice profiles. These profiles were constructed by fairing a curve through the "point" thickness measurements from the array transducers. A total of six profiles are shown, with six minutes between each profile. The time at which the profiles were measured is indicated on the lower plot of the cloud liquid water content during the flight.

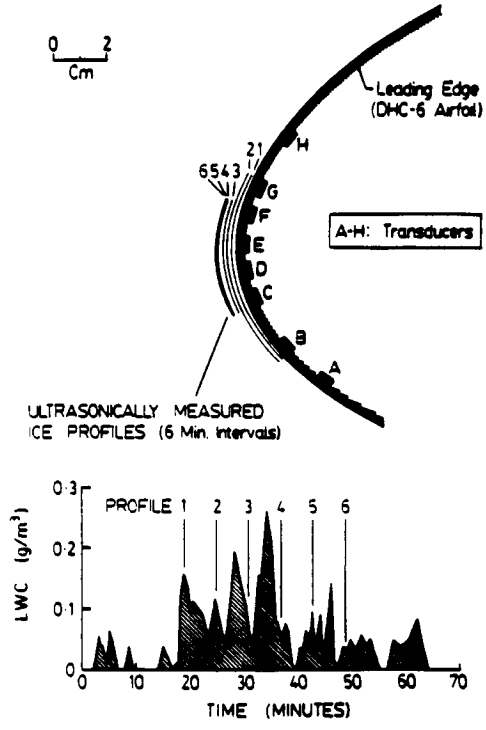

Fig. 23 Ultrasonically measured ice profiles for flight 86-31.

The ultrasonically measured profiles show the ice shape to be relatively conformable to the leading edge throughout the encounter. Thickness measurements from transducers B and G, located near the edges of the accretion, were not possible after the second profile. This was because the slope of the ice surface above these transducers, relative to the airfoil surface, became too large, reflecting the return echo away from the transducer and significantly reducing the received echo strength. Increasing the receiver gain in this situation would alleviate this problem; however, varying the receiver gain between transducers was not practical with the single multiplexed pulser/receiver used for these tests. Since a single "optimum" gain had to be used, this "edge" effect dropout of the echo signal was often unavoidable.

The ice profiles in Fig. 23 illustrate the non-uniform growth rate throughout the encounter. The first three profiles all show approximately equal growth, corresponding to the roughly constant average liquid water content during this period. The higher liquid water content in the interval between profiles 3 and 4 results in more growth, as evidenced by the larger profile spacing. Following profile 4 the liquid water content falls, and as a result profiles 5 and 6 show little further growth.

Fig. 24 illustrates the final ice shape accreted on the wing cuff at the completion of flight 86-31. Three separate measurements of the final ice profile are shown. The open circles represent thickness readings obtained from the stereo photographic analysis, while the crosses indicate measurements made with vernier calipers after landing. The final ultrasonic ice thickness measurements (from transducers C, D, E, and F) are shown as a solid line on the figure. The agreement between all three of these independent measurements is within 0.5 mm, with a final ice thickness of approximately 9 mm indicated.

5.0 CONCLUSION

In conclusion, ultrasonic pulse-echo measurement techniques are seen to offer the potential for the development of an operational ice detector, as well as providing a valuable tool for better understanding and documenting that ice accretion process.

ACKNOWLEDGMENTS

This work was supported by the National Aeronautics and Space Administration, the Federal Aviation Administration under the Joint University Program for Air Transportation, Grants NGL-22-009-640 and NAG-3-666, and the National Science Foundation Presidential Young Investigator Award Program. Wind tunnel and flight test facilities were provided by the NASA Lewis Research Center and the Boeing Commercial Airplane Company.

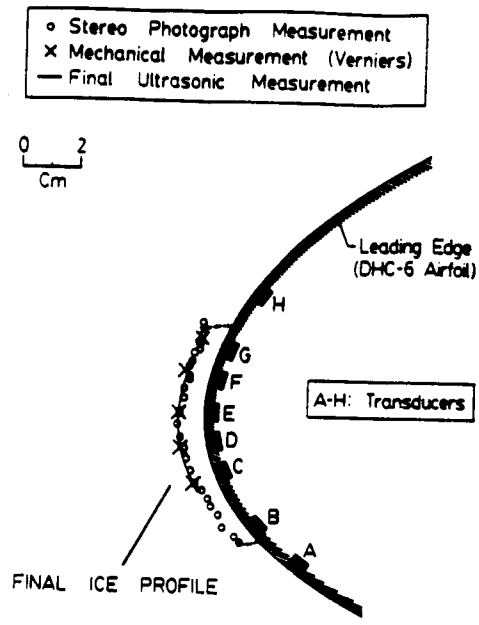

Fig. 24 Final ice profile for flight 86-31.

REFERENCES

1. Hansman, R.J. and Kirby, M.S., "Measurement of Ice Accretion Using Ultrasonic Pulse-Echo Techniques," *Journal of Aircraft*, Vol. 22, June 1985, pp. 530-535.

2. Van Fossen, G.J., et al., "Heat Transfer Distributions Around Nominal Ice Accretion Shapes Formed on a Cylinder in the NASA Lewis Icing Research Tunnel," AIAA-84-0017, January 1984.

3. Hansman, R.J. and Kirby, M.S."Comparison of Wet and Dry Growth in Artificial and Flight Icing Conditions" *Journal of Thermophysics and Heat Transfer*, Vol 1, July 1987, pp.215-227.

4. Hansman, R.J., Kirby, M.S., McKnight, R., and Humes R., "In-Flight Measurement of Airfoil Icing Using an Array of Ultrasonic Transducers," AIAA-87-0178, 1987.